

Line profiles in moustaches produced by an impacting energetic particle beam

M.D. Ding¹, J.-C. Héroux², and C. Fang¹

¹ Department of Astronomy, Nanjing University, Nanjing 210093, P.R. China

² Observatoire de Paris, DASOP-URA326 (CNRS), F-92195 Meudon Cedex, France

Received 1 October 1997 / Accepted 11 December 1997

Abstract. The $H\alpha$ line profile in moustaches is characterized by enhanced wings and a deep central absorption. We explore the possibility that such a profile may be due to the effect of energetic particles bombarding the atmosphere. Computations show that the characteristics of moustache line profiles can be qualitatively reproduced in two extreme cases, either injection from the corona of high energy particles ($\gtrsim 60$ keV electrons or $\gtrsim 3$ MeV protons) or injection in a low-lying site, in middle chromosphere or deeper, of less energetic particles (~ 20 keV electrons or ~ 400 keV protons). The requirements on the energy and on the depth of the injection site of energetic particles are reduced in the case of observations close to the solar limb. The rôle of protons of energies below 1 MeV is slightly less significant than that of deka-keV electrons in the case of a high particle injection site, but such protons remain to be viable candidates in the case of lower particle injection sites and of observations at larger heliocentric angles. Observations at various wavelengths are needed to find which of these hypotheses is convenient for explaining a given event.

Key words: line: profiles – Sun: activity – Sun: particle emission

1. Introduction

Moustaches, or Ellerman bombs, have been studied for several decades. Their spatial structure, lifetime, brightness, mass motion, and relationship to other solar activities were investigated by various authors (e.g., Engvold & Maltby 1968; Bruzek 1972; Kitai & Kawaguchi 1975; Kurokawa et al. 1982; Kitai 1983; Kitai & Muller 1984; Stellmacher & Wiehr 1991; Denker et al. 1995; Dara et al. 1997; Denker 1997). In particular, much effort has been devoted to the observations and theoretical interpretations of the peculiar line emissions in moustaches (e.g., Severny 1956, 1957, 1959; Engvold & Maltby 1968; Kitai 1983; Firstova 1986).

Send offprint requests to: M.D. Ding

A typical moustache line profile is characterized by enhanced and broadened line wings and a deep central absorption, examples of which can be found in Kitai (1983) for hydrogen Balmer lines and Severny (1956, 1957, 1959) for hydrogen and metallic lines. Several explanations for such broad emission profiles have been proposed. However, mechanisms invoking randomly directed macroscopic motions and electron scattering have been found not to be suitable (Kitai 1983).

Kitai (1983), using non-LTE calculations, computed the $H\alpha$ line profiles for various model atmospheres, which include a perturbed, heated and condensed, layer with constant ΔT and ρ/ρ_0 in the chromosphere. The computed profiles show that a model atmosphere with $\Delta T = 1500$ K and $\rho/\rho_0 = 5$ can well reproduce the observed $H\alpha$ profile. Kitai further argued that the condensed layer might be due to the upward propagation of a shock wave originating from below.

On the other hand, Firstova (1986) measured the linear polarization of $H\alpha$ and $H\beta$ lines in moustaches. The difference in the profiles obtained for two perpendicular directions of polarization cannot be interpreted in terms of Stark or Zeeman splitting. Firstova thus concluded that, similarly to the case of solar flares (Chambe & Héroux 1979; Héroux et al. 1983), the linear polarization of moustache lines is also likely to be produced by an energetic particle beam. Recently, Firstova et al. (1997) found that the $H\alpha$ line in moustaches is linearly polarized in the tangential direction, which can be interpreted as due to atmospheric bombardment by very energetic particles.

As the above attempts are focused on different aspects of the line profile, it is worthwhile to search for a mechanism that is responsible for both the line broadening and the polarization, though they are not necessarily produced by the same agent. Thermal models, such as that proposed by Kitai (1983), cannot explain the latter. Attention is therefore given to whether or not an atmosphere bombarded by an energetic particle beam can reproduce the observed line broadening and other features. The purpose of this work is to explore such a possibility.

2. Rôle of particle beams in the enhancement of line emission

2.1. Non-thermal excitation and ionization effect

An energetic particle (electron or proton) beam can heat the atmosphere through Coulomb collisions between the beam particles and the ambient atoms and ions. This process, together with heat conduction and to some degree X-ray irradiation, are thought to be key energy input processes in chromospheric flares. Fang & Hénoux (1983) presented theoretical flare models of the solar atmosphere heated by these processes, which show an obvious temperature rise in the chromosphere. However, a pure temperature rise would be insufficient to reproduce line profiles with broad wings.

Of significant interest is the study of another aspect of the effect of particle bombardment: collisional excitation and ionization of ambient atoms by beam particles. It has been shown that, such non-thermal excitation and ionization rates can be by orders of magnitude larger than the thermal collisional rates (Abouadarham & Hénoux 1986a, 1986b; Fang et al. 1993; Hénoux et al. 1993). Taking into account this non-thermal effect, only a sufficiently intense particle beam, without a very hot and condensed chromosphere, could reproduce the observed line broadening in flares (Fang et al. 1995b).

The above argument would be even more relevant in the case of moustaches, since a moustache line profile shows usually a central absorption, implying that the upper chromosphere is not heated greatly. Since moustaches and flares exhibit many similarities in their appearance and line emissions (Severny 1959; Koval 1965; Firstova 1986), non-thermal effects may also be at work in moustaches.

2.2. Rate of energy deposition by beam particles

For solar flares, the general point of view is that the energy release site lies in the corona and that the chromosphere is heated mainly by downward heat conduction or particle bombardment. This scenario may break down in explaining Type II white-light flares, in which the continuum emission is significantly enhanced but the line emission keeps relatively low. Instead, Li et al. (1997) proposed a mechanism which assumes that the magnetic reconnection occurs in the lower atmosphere (photosphere). If this is true, one would expect energetic particles to be produced there and then to be propagating both downwards and upwards. Based on this assumption, the energy release site will be regarded as an adjustable parameter in the following discussions.

We assume further that the particle production site is at a hydrogen column density N_0 and that equal fluxes of particles are ejected upwards and downwards. In the cold target approximation, the rate of energy loss for beam particles with column density N has the form (Emslie 1978; Hénoux et al. 1993):

$$\frac{dE}{d|N - N_0|} = -\frac{K}{\mu E} \gamma = -\frac{K}{\mu E} \frac{m}{m_e} [\xi \Lambda + (1 - \xi) \Lambda'], \quad (1)$$

where $K = 2\pi e^4$. In Eq. (1), m is the particle mass, μ is the cosine of the pitch angle, ξ is the ionization degree of the tar-

get, Λ is the Coulomb logarithm due to collisions with target electrons and protons, while Λ' the one from inelastic collisions with target atoms. The latter corresponds to the energy deposition contributed to the non-thermal excitation and ionization of target atoms. The rate for this part of energy deposition at column density N is written as (Emslie 1978; Chambe & Hénoux 1979):

$$\Phi = \frac{dE}{dt} = (1 - \xi) n_H \Lambda' \frac{m}{m_e} K \int_{E_N}^{\infty} \frac{F_0(E) dE}{E(1 - E_N^2/E^2)^{\frac{2+\beta}{4+\beta}}}, \quad (2)$$

where

$$E_N = \left[\left(2 + \frac{\beta}{2} \right) \frac{\gamma K |N - N_0|}{\mu_0} \right]^{\frac{1}{2}} \quad (3)$$

is the minimum energy of particles at N_0 that can penetrate to N . μ_0 is the cosine of the initial pitch angle and is taken to be unity throughout the paper. The expression for β can be found in Emslie (1978). Assuming that the flux spectrum for initial particles has a form of power law and a lower energy cut-off, we have

$$F_0(E) = \begin{cases} AE^{-\delta}, & E > E_1, \\ 0, & E < E_1, \end{cases} \quad (4)$$

where $A = (\delta - 2) \mathcal{F}_1 E_1^{\delta-2}$. \mathcal{F}_1 is the energy flux for particles propagating upwards or downwards only. Eq. (2) then reduces to

$$\Phi = \frac{1}{2} (1 - \xi) n_H \Lambda' \frac{m}{m_e} K (\delta - 2) \frac{\mathcal{F}_1}{E_1^2} \left| \frac{N - N_0}{N_1} \right|^{-\frac{\delta}{2}} \int_0^{u_1} \frac{u^{\frac{\delta}{2}-1}}{(1-u)^{\frac{2+\beta}{4+\beta}}} du, \quad (5)$$

where

$$N_1 = \frac{\mu_0 E_1^2}{(2 + \beta/2) \gamma K} \quad (6)$$

is the column density penetrated by particles with an initial energy E_1 , and

$$u_1 = \begin{cases} 1, & |N - N_0| > N_1, \\ |N - N_0|/N_1, & |N - N_0| < N_1. \end{cases} \quad (7)$$

What parameters can influence the rate of energy deposition? The energy flux, \mathcal{F}_1 , is clearly the most direct factor, but it can only change Φ in a proportional manner through the whole atmosphere. On the contrary, the power index, δ , can alter the height distribution of Φ . The lower energy cut-off, E_1 , has a similar but more pronounced effect. A smaller δ and/or a larger E_1 are needed for increasing the amount of energy deposition in the lower layers. Indeed such a requirement can also be achieved if we set a lower particle production site. Fig. 1 shows the variations of the rate of energy deposition obtained by changing either the lower energy cut-off or the particle production site.

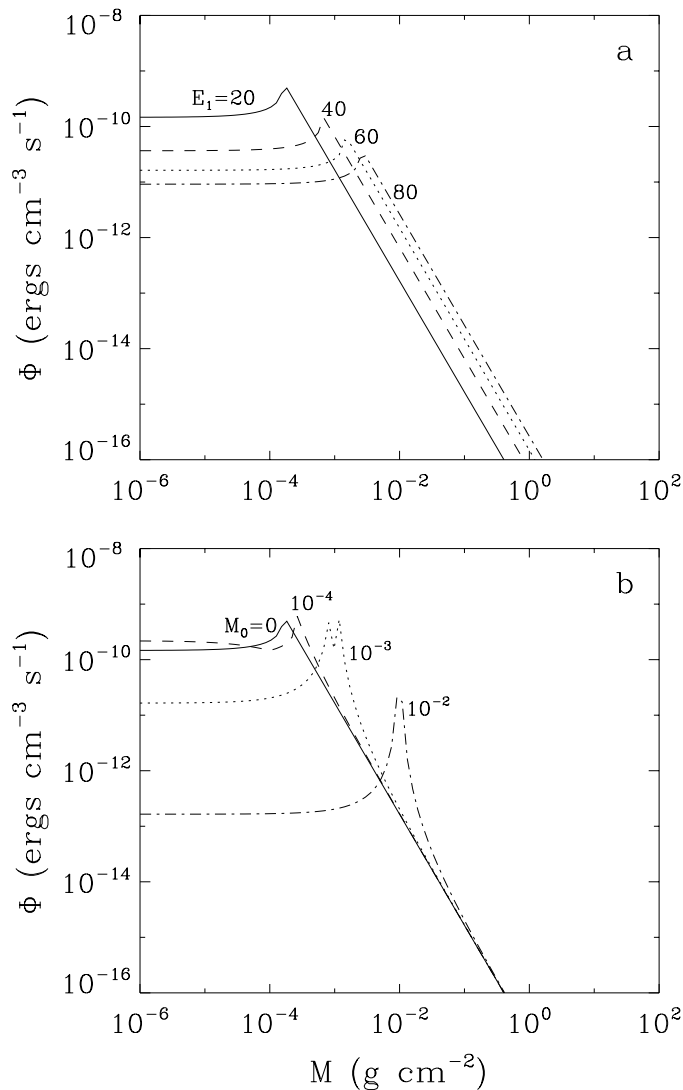


Fig. 1a and b. Rates of energy deposition in an atmosphere by electron beams. In all cases, the energy flux is $10^{11} \text{ ergs cm}^{-2} \text{ s}^{-1}$ and the power index is 4. **a** Electrons are injected from the corona ($M_0 = 0$). The lower energy cut-off is 20, 40, 60, and 80 keV for the four curves. **b** The lower energy cut-off is 20 keV. Electrons are injected from four sites corresponding to column mass densities $M_0 = 0, 10^{-4}, 10^{-3},$ and $10^{-2} \text{ g cm}^{-2}$

3. Effects of the various beam parameters on the $\text{H}\alpha$ line profile

In order to search for the most probable origin of moustache line profiles, we have to check the effects of all the possible factors described in Sect. 2.2 that can affect the rate of energy deposition. To do so, we employ the method used by Fang et al. (1993) and Hénoux et al. (1993). The rate of energy deposition in Eq. (5) is used to calculate the rates of non-thermal excitation and ionization of hydrogen atoms due to collisions with the particle beam (see Fang et al. 1993). These rates are incorporated into the statistical equilibrium equations and can substantially change the level populations of the hydrogen atom. Line pro-

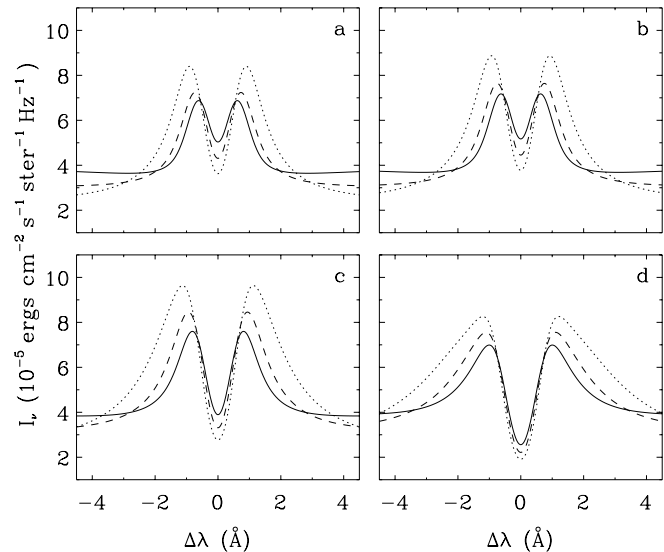


Fig. 2a–d. Computed $\text{H}\alpha$ line profiles from the model atmosphere F1 bombarded by an electron beam with $\mathcal{F} = 10^{11} \text{ ergs cm}^{-2} \text{ s}^{-1}$, $\delta = 4$, and $E_1 = 20 \text{ keV}$. The four panels correspond to different particle injection sites with column mass densities of **a** 0, **b** $1.7 \cdot 10^{-4}$, **c** $1.2 \cdot 10^{-3}$, and **d** $1.2 \cdot 10^{-2} \text{ g cm}^{-2}$. Solid, dashed, and dotted lines correspond to different heliocentric angles $\cos\theta = 1, 0.5,$ and 0.2 , respectively

files are finally calculated, with the line broadening from the Doppler effect, radiative damping, and pressure (van der Waals and Stark) effect taken into account.

We use the weak flare model F1 (Machado et al. 1980) as the base model for all the following computations. The reason for doing so is only, as mentioned in Sect. 2.1, the similarity between flares and moustaches. Of course, our purpose here is not to construct specific moustache models, but only to explore the rôle of energetic particles.

3.1. Effect of varying the height of particle production

As stated in Sect. 2.2, there is a possibility that the site of energy release in flares or moustaches does not lie in the corona but in lower layers. To investigate this effect on the line emission, we computed four cases in which energetic electrons are initially injected into the atmosphere from column mass densities $M_0 = 0, 1.7 \cdot 10^{-4}, 1.2 \cdot 10^{-3},$ and $1.2 \cdot 10^{-2} \text{ g cm}^{-2}$. These four cases correspond roughly to particle production sites in the corona, the upper chromosphere, the middle chromosphere, and the lower chromosphere, respectively. In all cases, the energy flux \mathcal{F} , the power index δ , and the lower energy cut-off E_1 are respectively $10^{11} \text{ ergs cm}^{-2} \text{ s}^{-1}$, 4, and 20 keV. The profiles of $\text{H}\alpha$ are presented in Fig. 2. Also shown in the figure are the center-to-limb variations of the profiles.

It is clear that when the site of particle production is set lower, the emission of $\text{H}\alpha$ line wings is more enhanced and, in particular, the central absorption of the line becomes more

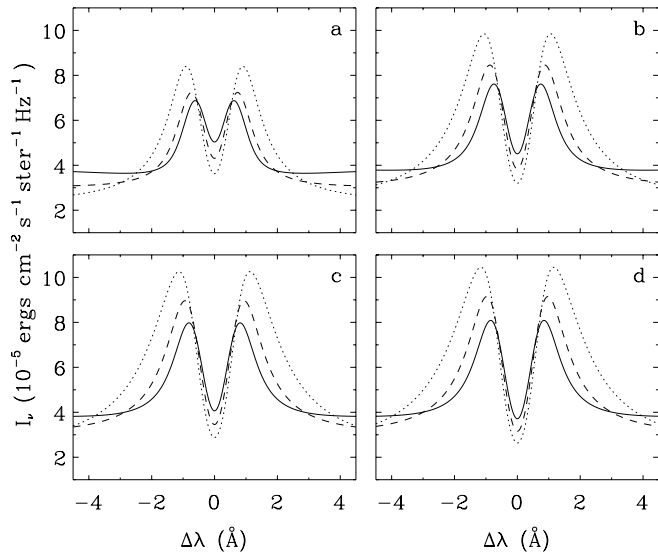


Fig. 3a–d. Computed $H\alpha$ line profiles from the model atmosphere F1 bombarded by electron beams with $\mathcal{F}_1 = 10^{11}$ ergs $\text{cm}^{-2} \text{s}^{-1}$ and $\delta = 4$. The four panels correspond to different lower energy cut-off E_1 of **a** 20, **b** 40, **c** 60, and **d** 80 keV. Electrons are injected from the corona ($M_0 = 0$). Solid, dashed, and dotted lines correspond to different heliocentric angles $\cos \theta = 1, 0.5$, and 0.2 , respectively

obvious. The latter is characterized by a lower core intensity, as well as a larger peak separation.

Theoretical explanation for the above results is simple. The non-thermal excitation and ionization of the hydrogen atom raise the $H\alpha$ source function. With a lower site of particle production, more energy is deposited in the lower chromosphere where the wings are formed while less energy goes to the upper chromosphere where the line center originates.

It is worth noting that the profiles have been convolved with a Gaussian macro-turbulent velocity of 20 km s^{-1} . Like in the case of flares, this is used to mimic the seeing effect on unresolved structures in which macroscopic velocities may be distributed randomly. Adopting a different macro-turbulent velocity only changes the contrast of peak and core intensities. It does not affect the qualitative behaviour of the profile.

3.2. Effect of varying the lower energy cut-off

As indicated in Sect. 2.2, another factor that can cause more energy to be deposited in lower layers is an increase of the lower energy cut-off, E_1 , of the particle beam. We now adopt the classical point of view that the particle beam is injected into the atmosphere from the corona ($M_0 = 0$). Four cases corresponding to electron beams characterized respectively by $E_1 = 20, 40, 60$, and 80 keV have been considered. The energy flux \mathcal{F}_1 and the power index δ are still set to be 10^{11} ergs $\text{cm}^{-2} \text{s}^{-1}$ and 4 . The resulting line profiles of $H\alpha$ are shown in Fig. 3.

The effect of raising the lower energy cut-off is qualitatively similar to the effect of lowering the height of particle production. That is to say, even though the particles are originally produced

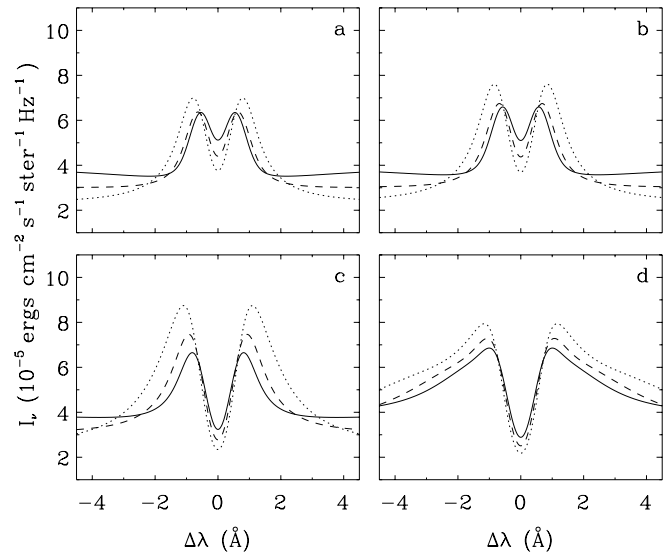


Fig. 4a–d. Computed $H\alpha$ line profiles from the model atmosphere F1 bombarded by a proton beam with $\mathcal{F}_1 = 10^{11}$ ergs $\text{cm}^{-2} \text{s}^{-1}$, $\delta = 4$, and $E_1 = 400$ keV. The four panels correspond to different particle injection sites with column mass densities of **a** 0, **b** $1.7 \cdot 10^{-4}$, **c** $1.2 \cdot 10^{-3}$, and **d** $1.2 \cdot 10^{-2}$ g cm^{-2} . Solid, dashed, and dotted lines represent different heliocentric angles $\cos \theta = 1, 0.5$, and 0.2 , respectively

in the corona, if they can be accelerated to an energy higher than generally thought, they can still deposit a significant amount of energy in the deep atmospheric layers to raise the line source function there without affecting too much the top layers. Of course, the power index of the particle beam has also some influence on the height distribution of the energy deposition rate, but comparatively it is a minor factor.

3.3. Center-to-limb variation

Figs. 2 and 3 also show the center-to-limb variation of the profile. Under the same condition, profiles near the disk limb exhibit a more intense inner wing and a more pronounced central absorption than in the disk center case. Therefore, it seems to be easier to generate a moustache profile at large heliocentric angles.

3.4. Electrons or protons?

In solar flares, electrons have been regarded as the main constituent of energetic particles that transport energy during the flare impulsive phase. Recently, there was a hot debate when it was suggested that protons may play the chief rôle, while the rôle of electrons is only secondary (Simnett 1995). Emslie et al. (1996) showed that 1 MeV protons deposit energy in a manner similar to 20 keV electrons.

In the case of moustaches, there is much less observational evidence than for flares to ascertain which kind of particles are dominant. To check the rôle of protons, we computed profiles associated with a proton beam characterized by $\mathcal{F}_1 = 10^{11}$ ergs $\text{cm}^{-2} \text{s}^{-1}$, $\delta = 4$, and $E_1 = 400$ keV, and injected into the

atmosphere from the same four heights as in Fig. 2. The results are plotted in Fig. 4. Fig. 4 shows that, if the particle production site lies high in the atmosphere, 400 keV protons are even less effective in producing the wing emission and central absorption of the H α line than 20 keV electrons. However, if the particle production site is lower enough, and/or the event occurs near the disk limb, such protons play a similar rôle to that of electrons, so that they may still be regarded as viable candidates to produce moustache line profiles.

It can be seen from Eq. (5) that the heating effect of protons would be equivalent to that of electrons, if the energy of the former reaches $(m_p/m_e)^{1/2}$ times the energy of the latter (see Emslie et al. 1996). Therefore, line profiles associated with 20–80 keV electrons (Fig. 3) would nicely be reproduced in the case of 1–4 MeV protons. This point has been confirmed in computations.

4. Conclusions

In all the computations presented above, we have fixed the model atmosphere and the energy flux of particle beams. Even so, the computed H α profiles (e.g., those in panel d of Fig. 2) match fairly well the observed ones shown in Kitai (1983), with only a slight difference in the contrast of peak and core intensities. However, this difference can be reduced by changing the parameters of particle beams, the model atmosphere, and the macro-turbulent velocity. Further spectral observations of moustaches are needed in order to carry out detailed model computations.

We have considered mainly the general behaviour of the H α line profile in the presence of energetic particles. A typical moustache profile, characterized by enhanced wings and a deep central absorption, can be qualitatively reproduced in two extreme cases either by injection from the corona of particles with very high energies ($\gtrsim 60$ keV electrons or $\gtrsim 3$ MeV protons) or by injection of less energetic particles (~ 20 keV electrons or ~ 400 keV protons), in a low-lying site located in the middle chromosphere or deeper. In these two cases, the heating (non-thermal excitation and ionization) effect mainly occurs in the deeper layers where the line wing emission is formed, while the upper layers are kept relatively cooler, which can account for the central absorption of line profiles. A center-to-limb variation of the resulting profile is also obvious. The requirements on the particle energy and on their depth of injection are strongly reduced in the case of observations made close to the solar limb. The rôle of protons of energies less than 1 MeV is slightly less significant than that of deka-keV electrons in the case of a high particle injection site, but such protons remain to be viable candidates in the case of lower injection sites and larger heliocentric angles.

If beam protons are present in the moustache atmosphere, the charge exchange between protons and ambient hydrogen atoms would lead to Doppler-broadened hydrogen lines (Canfield & Chang 1985; Fang et al. 1995a). In particular, the broadening and asymmetry of the line profiles depend strongly on the proton pitch angle and the inclination between the line of sight and the magnetic field (Zhao et al. 1997). Therefore, we cannot

exclude that in some special cases, protons of energies of a few hundred keV could also contribute to some extent in the line broadening in moustaches through charge exchange.

The observation of tangential linear polarization in moustaches (Firstova et al. 1997) indicates that protons of energies higher than 200 keV or electrons of a few ten keV are present, moving vertically in the H α line forming layer. However neither polarization observation nor moustache line profiles can distinguish what kinds of particles are present. Detailed comparison between computed and observed profiles may refine the diagnostic, but would presumably not close the debate. Therefore other observational tests are needed. Observations of the hard X-ray and γ -ray spectra with high sensitivity instruments may give the clue.

On the other hand, although magnetic reconnection in deeper layers, leading to particle acceleration, is theoretically possible (Li et al. 1997), it still lacks direct observational evidence. The observation of lines and continua formed at various depths would provide useful information. Particle beams could enhance the hydrogen continuum emission. As Lyman, Balmer, and Paschen continua are formed at quite different depths, they can be used to diagnose the height distribution of the energy deposition by beam particles.

In conclusion, in order to investigate in more detail the origin of moustache lines, observations should be performed in various spectral ranges, including both lines and continua in the visible range.

Acknowledgements. Part of this work was done during M.D.D. visited Paris Observatory. He would like to thank the Observatory for financial support and kind hospitality. This work was partly supported by funds from the National Natural Science Foundation of China and from the Centre National de la Recherche Scientifique of France.

References

- Aboudarham J., Hénoux J.-C., 1986a, *Adv. Space Res.* 6(6), 131
- Aboudarham J., Hénoux J.-C., 1986b, *A&A* 168, 301
- Bruzek A., 1972, *Solar Phys.* 26, 94
- Canfield R.C., Chang C.-R., 1985, *ApJ* 295, 275
- Chambe G., Hénoux J.-C., 1979, *A&A* 80, 123
- Dara H.C., Alissandrakis C.E., Zachariadis Th.G., Georgakilas A.A., 1997, *A&A* 322, 653
- Denker C., 1997, *A&A* 323, 599
- Denker C., de Boer C.R., Volkmer R., Kneer F., 1995, *A&A* 296, 567
- Emslie A.G., 1978, *ApJ* 224, 241
- Emslie A.G., Hénoux J.-C., Mariska J.T., Newton E.K., 1996, *ApJ* 470, L131
- Engvold O., Maltby P., 1968, in: Öhman Y. (ed.) *Mass Motions in Solar Flares and Related Phenomena*, Nobel Symp. 9, 109
- Fang C., Feautrier N., Hénoux J.-C., 1995a, *A&A* 297, 854
- Fang C., Hénoux J.-C., 1983, *A&A* 118, 139
- Fang C., Hénoux J.-C., Gan W.Q., 1993, *A&A* 274, 917
- Fang C., Hénoux J.-C., Hu J. et al., 1995b, *Solar Phys.* 157, 271
- Firstova N.M., 1986, *Solar Phys.* 103, 11
- Firstova N.M. et al., 1997, *A&A*, in preparation
- Hénoux J.-C., Chambe G., Semel M. et al., 1983, *ApJ* 265, 1066
- Hénoux J.-C., Fang C., Gan W.Q., 1993, *A&A* 274, 923
- Kitai R., 1983, *Solar Phys.* 87, 135

- Kitai R., Kawaguchi I., 1975, *Solar Phys.* 44, 403
Kitai R., Muller R., 1984, *Solar Phys.* 90, 303
Koval A.N., 1965, *Izv. Krymsk. Obs.* 33, 138
Kurokawa H., Kawaguchi I., Funakoshi Y., Nakai Y., 1982, *Solar Phys.* 79, 77
Li X.Q., Song M.T., Hu F.M., Fang C., 1997, *A&A* 320, 300
Machado M.E., Avrett E.H., Vernazza J.E., Noyes R.W., 1980, *ApJ* 242, 336
Severny A.B., 1956, *Izv. Krymsk. Obs.* 16, 194
Severny A.B., 1957, *Izv. Krymsk. Obs.* 17, 129
Severny A.B., 1959, *Izv. Krymsk. Obs.* 21, 131
Simnett G.H., 1995, *Space Sci. Rev.* 73, 387
Stellmacher G., Wiehr E., 1991, *A&A* 251, 675
Zhao X., Fang C., Hénoux J.-C., 1997, *A&A*, in press